Geochemical study of products associated with spontaneous oxidation of coal in the Cerro Pelado Formation, Venezuela

M. Martínez [a], G. Márquez [b], F.J. Alejandre [c,*], J.J. Del Río [c], A. Hurtado [a]

[a] Instituto de Ciencias de la Tierra, Universidad Central de Venezuela, Caracas, 3895, 1010-A, Venezuela
[b] Departamento de Ingeniería Minera, Mecánica y Energética, Univ. de Huelva, Palos de Fra., 21819 Huelva, Spain
[c] Departamento de Construcciones Arquitectónicas II, Universidad de Sevilla, Reina Mercedes n° 4, 41011 Sevilla, Spain

ARTICLE INFO

ABSTRACT

The aim of this research work is a geochemical, mineralogical, and textural characterization of spontaneously smouldered coal-derived products in northwestern Venezuela (Cerro Pelado Formation, some 10 km from Pedregal city). Several solid samples were collected from this formation, six of unweathering coal, an other six of resulting unmelted rocks forming on a surface coal bed, and the last four of mineralizations found accumulating around gas vents. The fresh coal and the unmelted material were analysed by scanning electron microscopy, X-ray diffraction, and proximate techniques. Products such as magnetite and chabazite-K were identified in the alteration rocks. Likewise, both materials were also studied in order to determine the mobilization of 17 elements into the environment; such elements were analysed through inductively coupled plasma atomic emission spectroscopy on extracts obtained by a sequential extraction method: each sample was firstly extracted with MilliQ water and then the resultant residue was washed. This and the subsequently resulting residues are extracted according to the mentioned procedure by using, respectively, ammonium acetate, chlorhydric acid, peroxide and chlorhydric acid, nitric acid and fluorhydric acid, and nitric acid. The studied elements are classified as highly mobile (Na, Ni, ...), nearly immobile (Ti, P) and partially mobile (Mg, Fe, K, ...). In regards to mineralizations around fumaroles associated with smoldering coal seams, Fourier-transform infrared spectroscopy and X-ray diffraction analyses have revealed the presence of salammoniac, mascagnite and other solid combustion compounds formed by reaction of gas emitted from coal oxidation, in addition to previously non-reported sulfur-rich by-products associated with gas fissures, particularly ammonium thiosulfate, a phase first obtained only synthetically in the laboratory. Another objective of the research was to collect and analyse gases escaping from surficial vents. Relatively high concentrations of several aromatic compounds were detected in the gas collected at the studied coal outcrop, as well as aliphatic hydrocarbons including ethane, propane, butanes, among others. High contents of carbon monoxide, methane and carbon dioxide were also measured for gas samples.

© 2009 Elsevier Ltd. All rights reserved.

1. Introduction

This study describes and analyses the principal oxidation products formed by smoldering coal beds in the Cerro Pelado Formation (Venezuela). The primary objectives of this research were to characterise fresh materials, clinkers and fumarolic mineralizations produced by spontaneous oxidation in an outcrop of sulfur-nitrogen-rich coal, along with 17 chemical elements (minor and trace constituents of coal; Finkelman, 1999) released from coal in different grades. The behaviour of these elements in the process of self-oxidation is studied based on their concentrations in the extracts derived from both fresh coal and clinker samples after the sequential attack by various reagents. Another objective was to detect

new and unclassified fumarolic mineralizations formed as reaction products of gas emitted from the mentioned outcrop of coal in order to better understand of the effects of high sulfur and nitrogen contents on the geochemistry of smoldering coal beds. This work also contributes to document the main compounds present in gaseous effluents associated with hot fumaroles.

Under certain natural conditions, a coal bed in contact with air may spontaneously oxidise, resulting in an exothermic process termed spontaneous combustion. This phenomenon can turn the bed of fresh coal into a suite of thermally metamorphosed rocks – known as clinkers – formed by heating and chemical alteration of sedimentary rocks during oxidation of underlying coal beds (Sarnecki, 1991; Coates and Heffern, 2000). This process is also characterized by the emission of different gases and particulate matter (Stracher and Taylor, 2004). Likewise, some mineralizations associated with fumaroles have resulted from the interaction of gas

* Corresponding author. Fax: +34 954556691.
  E-mail address: falejan@us.es (F.J. Alejandre).

jets and mineral phases along with surface water and surrounding rocks. The bituminous coal is inclined to spontaneous burning, and any outcrop of fresh coal is likely to burn spontaneously if exposing to the air by landslide, or rapid erosion (Lyman and Volkmer, 2001). This process is induced either by coal fines, or by exothermic reactions catalyzed by oxygen circulating through high-sulfur coal seam joints (Anthony et al., 1977).

The mechanisms of spontaneous oxidation of coal have been extensively studied (Kaymakci and Didari, 2002; Stracher et al., 2004; Chaterjee, 2006; among others), and are shown here. The interaction of coal with air and/or moisture depends on a series of adsorptive, absorptive and chemical processes (Hudak, 2002) and the physico-chemical characteristics of the coal (Ceglarska-Stefanska et al., 1998). The main low temperature processes leading to self-oxidation of coal are physical and chemical absorptions of oxygen to form different unstable compounds known as peroxy-complexes and generate heat as a by-product of the modified surface energy of the material (Rosema et al., 2001). These processes cause an initial rise in temperature if conditions are just right for adequate air flow of the coal, neither too high, as the heat generated would be dissipated, nor too low, which would impede the coal-oxygen interaction (Chakravorty and Kolada, 1988). At the self-heating point or minimum temperature – approximately 70 °C – at which the material burns spontaneously, the peroxy-complexes decompose at an accelerating rate to provide oxygen for the oxidation process (Banerjee, 1985). As the temperature of coal rises, the peroxy-complexes decompose at a rate greater than they form (Wang et al., 2003) and gaseous products of exothermic reaction appear. Finally, when temperature exceeds 150 °C, the oxidation rate increases rapidly in the later stages of the burning process until spontaneous combustion occurs (Stracher et al., 2004).

Coal-fire beds are relatively common in tropical areas, where high atmospheric humidity means dense air stays low to the ground, maintaining contact with the coal bed. In these conditions, moisture fixation and finely divided pyrite or marcasite is very important (León, 1992). Ferrous pyrite oxidises at ambient temperatures in humid air, producing ferrous sulfate and sulfuric acid through the following reactions that exemplify the fact that moisture is also leading to spontaneous burning (Limacher, 1963):

$$2FeS_2 + 7O_2 + 2H_2O = 2H_2SO_4 + 2FeSO_4 + Heat$$
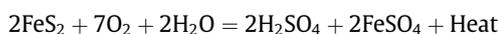
The ferrous ion has a catalytic effect on spontaneous coal oxidation (Carras and Young, 1994). Where seams are scarcely or not at all pyritic, self-oxidation may be the result of the hygroscopic nature of the coal, which tends to readsorb or gain humidity from the air as atmospheric vapour. This humidifying process can be even more exothermic than the results of pyrite oxidation. Humidity also has the effect of fracturing the coal and thus granting better access to air; furthermore, oxygen dissolved in water is more active (Walker, 1999).

In the state of Falcon in Venezuela is an interesting outcrop of coal unstudied until now (Fig. 1a). It has been spontaneously smoldering for several years, emitting hot gases accompanied by the precipitation of unusual altered materials. Moreover, the coal material does not undergo rapid self-oxidation; rather it constantly dissipates the heat produced (Glasser and Bradshow, 1990). This coal bed, approximately 60 cm thick, is located in "La Cuesta" mine (coordinates equal to 11°04′43″N, 70°12′41″ W) near the city of Coro in the Cerro Pelado Formation (Fig. 1b). The outcrop, about 40 m², contains ten vents, three over 50 cm in diameter and the others less than 20 cm in diameter. On the edges of the vents and in their vicinity appear fumarolic mineralizations.

The coal ignites and smoulders outside into a slope, for as long as it is able to draw in air, then goes out when fractures fail to reach the surface or the fire reaches the level of the water table in the coal outcrop. The front part of the clinker mass is attacked and removed by erosion, permanently exposing more coal, which ignites and forms more clinker material (Heffern and Coates, 2004). As a consequence, the clinker material is highly fractured, which allows air and moisture to enter and gas jets to escape, so that the oxidation processes continue (Coates, 1991). Gases emitted from vents in coal outcrops consist of a complex mixture of greenhouse gases, hydrocarbons, hydrogen sulphide, argon, carbon monoxide, water vapour, oxides of sulfur and nitrogen, and others that are associated with negative effects on environment and on human health (Finkelman, 2004). The presence of these products in the gas samples may be explained by the thermal degradation during spontaneous oxidation process of biopolymers buried in the coal seams (Puttmann et al., 1991).

2. Geological setting

The Falcón Basin is located in northwestern Venezuela, comprising several states of this country: the whole of Falcón and partially Zulia, Lara and Yaracuy (Audemard et al., 1999). This is a Tertiary basin, with a sediments volume approximately of 161,000 km³ and an extension of 36,000 km² (González de Juana et al., 1980). The Falcón Basin has also a suitable position in northwestern South America, occurring in the interaction zone between several major plates – Caribbean, Nazca and South America – and minor lithospheric blocks: Maracaibo, Bonaire and Western Colombia. Its sedimentary record, except various unconformities of regional extent, is almost continuous since the late Eocene (Audemard, 2003).

The Falcón Basin is the Venezuelan basin with the smallest volumes of liquid hydrocarbons, but it shows significant gas reserves and coal deposits. In this basin, several stratigraphic units contain organic matter (Boesi and Goddard, 1991). One of them is the Cerro Pelado Formation (Miocene) deposited during a marine transgression, and made of an alternation of thin layers of lutites with limestones and sandstones representing a turbiditic sedimentation (Díaz de Gamero, 1977).

The Cerro Pelado Formation, a sedimentary unit around 1500 m thick, extends throughout the south-central part of Falcón State in Venezuela (González de Juana et al., 1980). The unit primarily consists of lithic sandstones in beds up to 20 m thick intercalated with lutite and limonite beds with a maximum thickness of 2.7 m (Díaz de Gamero, 1977).

The bottommost part of the unit is grey to reddish-brown ferruginous sandstones with cross-bedding. Upsection are calcareous sandstones with bedding planes containing coal beds up to 2 m thick (Díaz de Gamero and Linares, 1989). Lutites are sometimes carbonaceous and contain greyish-blue limestone nodules; in addition, they contain fossils primarily typical of brackish waters from which the formation has been dated as Miocene (Hambalek et al., 1994).

These coal beds were deposited in a marine sedimentary environment with lagoons and marshlands that developed due to delta advancement, and the coal (sub-bituminous to bituminous) is found in the middle and upper part of the Cerro Pelado Formation (González et al., 1985). Inorganic material occurs in variable proportions and total sulfur contents are high, generally over 2% (González et al., 1985).

3. Materials and methods

Random sampling was carried out of fresh coal, clinkers, and mineralizations in the vicinity of several gas vents. Sampling trenches (Gleit, 1986) were dug to a length of 25 m with 1 m between adjacent trenches. We hand-collected the following sam-
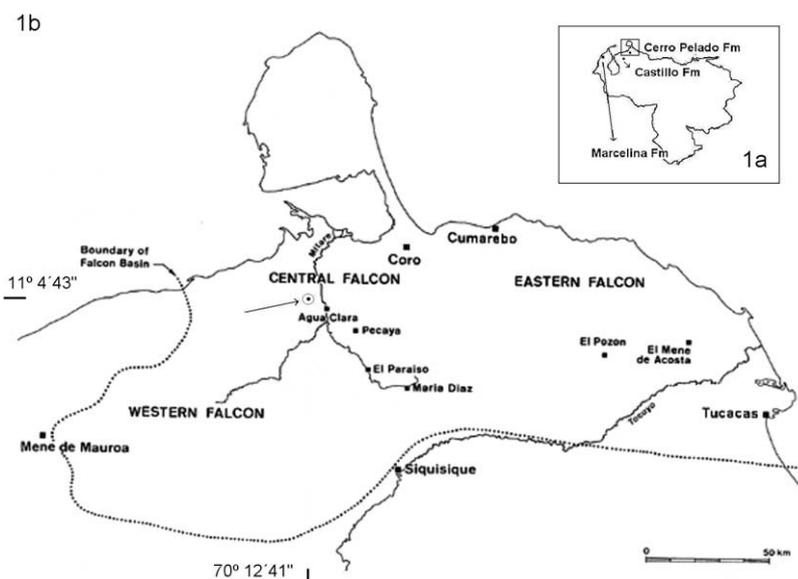
Fig. 1. (a) Location of several burning coal sites in Venezuela (Cerro Pelado, Castillo and Marcelina formations); (b) Situation (black circle) of the study site in the Falcón Basin.

ples: around 600 g of fresh, bright black coal with an average specific gravity of 1.5 and an average Mohs hardness of 0.4; about 500 g of unmelted material that was very friable and powdery; and approximately 200 g of mineralizations found accumulating around gas vents. Six samples of clinkers, an equal number of unaltered coal, and four of fumarolic mineralizations were homogenised then put through a Jones jaw crusher to obtain 100 g of each. An Etrex GPS was used to record coordinates of the study outcrop.

The clinker and fresh coal samples were analysed for moisture, volatile matter, ashes, and fixed carbon (in accordance with standards ASTM D-3172-89; ASTM International, 2002). The first three parameters were determined by weight difference by heating 10 g of sample; the fixed carbon was calculated by subtracting the sum of the other three parameters from the total (100%). Moisture was determined by heating the sample for 1 h at 110 °C (standard ASTM 3173-03). Volatile matter was heated for 7 min at 950 °C (standard ASTM 3175-02) and ash for 4 h at 750 °C (ASTM 3174-02). Last, the percentage of total sulfur was calculated on 0.5 g of sample in a LECO SC-432 analyser at 1350 °C for 6 min (standard ASTM 2492-02). Quantification of carbon, hydrogen, and nitrogen contents were carried out using a CARLO ERBA 1106 elemental analyser (Martínez et al., 2001).

Chemical analyses of 17 minor and trace elements were determined by inductively coupled plasma atomic emission spectroscopy technique (ICP-AOS) on aqueous extracts obtained by the sequential attack of a series of reagents on 10 g samples of clinker and fresh coal. A Perkin Elmer Optima 3000 sequential spectrometer equipped with an automatic sampler was used. Specifically, the following sequence of extractants was used for 30 min at ambient temperature: 50 ml of MilliQ water, 50 ml of 1 M aqueous solution of ammonium acetate, 50 ml of 1 M chlorhydric acid, 50 ml of an aqueous solution of 11% hydrogen peroxide and 0.7 M chlorhydric acid, and 15 ml of 70% nitric acid. Finally, 15 ml of an aqueous solution of 30% fluorhydric acid and 27% nitric acid was used for 24 h at 100 °C. This six-step method is a modification of previous procedures (Palmer et al., 1993; McCarty et al., 1998; among others). Accuracy of the sequential method for unaltered coal analysis was tested with SARM 19 standard. In contrast, no certified material comparable the clinker examined in this study could be found.

Trace and minor element composition of the fresh coal and clinker were determined through X-ray fluorescence spectroscopy using an energy-dispersive X-ray Panalytical spectrometer, model Axios, equipped with a digital signal processor and dual multi-channel analyser.

The surface texture was examined by using a scanning electron microscopy. A Jeol JSM 6460-LV microscope was used. SEM images in back-scattered electron mode (BSE) were acquired using several gold-plated pieces of sample.

The mineralogical composition was studied in the solid samples by powder X-ray diffraction (XRD) using a Bruker-AXS D8 Advance diffractometer equipped with a copper filament, Cu Kα radiation, tube conditions of 40 kV and 30 mA, fixed slot and sparkle detector. The diffractograms were obtained using the powder technique. XRD patterns in 2θ range 10–70° were acquired applying a 0.05° step scan with a 1 s step time. Subsequently, a sample of unaltered coal was analysed in a 10–70° 2θ scanning area using a 0.05° step scan with a 3 s step time.

Fourier-transformed infrared spectroscopy (FTIR) was used in order to determine the mineralogical composition of the fumarolic mineralizations through a Bomen spectrophotometer, model MB-120, using 4 cm^{-1} resolution and spectra recorded between 4000 and 400 cm^{-1}.

Gas samples were collected from the studied coal outcrop using vacuum stainless steel canisters. The gas was pumped into a container for storage and transported to the laboratory for analysis. In addition, the vent temperature was measured using a digital thermocouple connected to a 1.0 m platinum thermoprobe.

Gas chromatographic analyses of the gas samples were performed through a specific method (Colman et al., 2001; Barletta et al., 2002). The analytical techniques involved the cryogenic pre-concentration of each sample with liquid nitrogen (-196 °C). The pre-concentrated gas was later vapourised using a hot water bath and split into different detectors connected to two separate Hewlett-Packard 5890 gas chromatographs (GC). A mass spectrometer detector (MSD) and a flame ionization detector (FID) were both used to analyse hydrocarbons. Carbon monoxide and methane were analysed using a GC equipped with FID. For carbon dioxide, a thermal conductivity detector was used. Water vapour was not quantified because of its propensity to condense in the canister and its variability in coal-fire gas (Pone et al., 2007).

4. Results and discussion

4.1. Chemical and proximate analyses

The unmelted substrate samples comprised 95.2% ash by weight and 9.5% sulfur by weight; both values are well above the average for fresh coal from the Cerro Pelado Formation, which gives averages of 1.9% and 2.1%, respectively. In contrast, the clinker material contains 2.0% fixed carbon as opposed to 54.0% by weight in the unaltered coal. Moisture, on the other hand, is 1.8% for fresh coal and 2.8% for clinkers (see Table 1 for all these results). This table also shows average values for elemental analyses of studied samples.

As can be seen, a comparison of the clinker material with the data for the fresh coal clearly shows that, not surprisingly, the former has almost no volatile matter and a very high percentage of ash. This substantial drop in the percentage of fixed carbon in the clinkers is an unequivocal indication that oxidation destroys nearly all of the organic material in the coal. In addition, a series of volatile components are released (carbon monoxide, anhydrous carbon, methane, ethane, and others) with a consequent enrichment in the mineral fraction in the unmelted substrate.

The concentrations of 17 elements (Si, Al, Ti, Na, Mg, Ca, K, Cr, Zn, P, Mn, V, Cu, Ni, Sr, Ba, and Fe) were determined in the extracts derived from both unaltered coal and clinker material. The presence of a specific element in each extract serves to relate it to its corresponding compounds. Thus, the soluble salts occluded in the organic matter are associated with an attack by MilliQ water; the exchangeable ionic species adsorbed with the aqueous dissolution of ammonium acetate: labile substances (carbonates, and others) present in the coal with chlorhydric acid; the oxidative compounds associated with organic matter are related to the dis-

solution of peroxide and chlorhydric acid; the species derived from the digestion of refractory phases (sulfur and others) with nitric acid; and finally, the substances deriving from silicate digestion are related to the dissolution of fluorhydric acid and nitric acid.

Tables 2 and 3 summarise the concentrations of the 17 elements mentioned in the aqueous extracts obtained for the fresh coal and for the clinker samples. Significant differences in element concentrations were demonstrated ($P < 0.04$) by using t-test for both types of samples; thus it is not acceptable to hypothesise that the two sets of values are the same. This statistical analysis was performed using the SPSS 13.0 package for Windows.

The results show that spontaneous burning in the study coal outcrop causes a significant lowering in the concentrations of Na, Sr, Si, Cu, Ni, and Zn, suggesting these elements are lixiviated during oxidation. These elements are primarily associated with clay minerals and oxidizing compounds in unaltered coal (Bouska, 1981), but not in clinker material. This shift indicates that the majority of these minerals pass to an aqueous solution, almost entirely mobilising to form hydrosoluble species (Pone et al., 2007).

There is also a relative enrichment in other minerals (Fe, Cr, Mg, Ba, Ca, Mn, Al, K, and V) in the aqueous solutions when comparing fresh coal with clinker, indicating that they are only partially lixiviated during self-oxidation. However, the last four elements (Mn, Al, K, and V) also increase several fold in silicates and refractory phases in the transformation from unweathered coal to clinker material (Escobar and Martínez, 1993).

Finally, there is nearly a 50-fold increase in the P and Ti concentrations from fresh coal to clinker (approximately the same ratio by which the coal is reduced in mass due to the spontaneous oxidation) as a result of enrichment due to loss of organic matter. In both unaltered coal and clinker, P and Ti are primarily associated to silicates and refractory phases (Escobar and Martínez, 1993).

Fig. 2 displays the percentages of total extracted from fresh coal and clinker samples for each element during the six-step sequential method. In order to determine the effectiveness of the method for extracting elements, a total percent recovery value was calculated. For each element, the total concentrations obtained from bulk analyses for clinker material and fresh coal were compared to the total concentrations extracted by the method; recoveries were about 90% and 80%, respectively.

4.2. Scanning electron microscopy

SEM analysis in back-scattered electron (BSF) mode of the clinker material reveals a series of needle-like and pneumatolytic

Table 1
Proximate and elemental analyses of fresh coal and clinker samples. All data expressed in percentages (%).

Sample	Fresh coal	Altered material
Ash weight	1.9	95.2
Volatile matter	42.3	0.0
Fixed carbon	54.0	2.0
Moisture	1.8	2.8
Sulfur	2.1	9.5
Nitrogen	1.9	0.1
Carbon	82.5	2.1
Hydrogen	5.2	0.4

Table 2
Average Si, Ti, Na, Mg, Ca, K, Cr, Zn, P, Mn, V, Cu, Ni, Sr, Ba and Fe contents (ppm) of aqueous extracts obtained from unaltered coal.

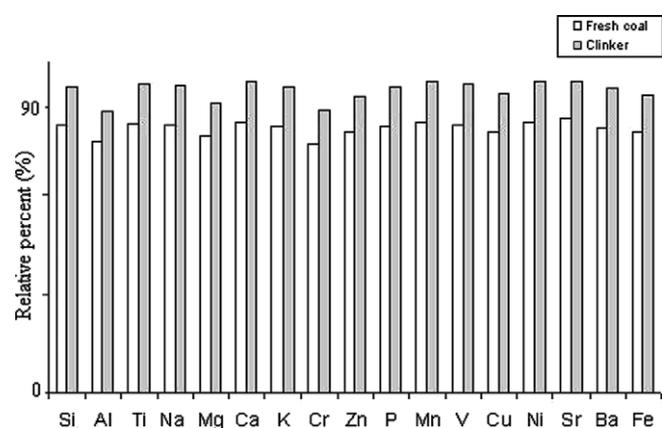|	MilliQ	Acetate	HCl	HCl-H$_2$O$_2$	HNO$_3$	HF-HNO$_3$
Si	0.00	0.00	0.00	50 ± 6	0.00	1364 ± 210
Al	121 ± 20	45 ± 7	32 ± 5	52 ± 7	280 ± 31	32 ± 6
Ti	0.00	0.00	0.70 ± 0.10	3.0 ± 0.4	0.00	61 ± 7
Na	52 ± 8	21 ± 3	38 ± 5	163 ± 22	139 ± 19	191 ± 25
Mg	281 ± 29	52 ± 6	42 ± 5	23 ± 3	104 ± 11	103 ± 10
Ca	86 ± 9	59 ± 8	106 ± 13	64 ± 8	120 ± 14	173 ± 20
K	25 ± 3	72 ± 8	144 ± 16	74 ± 9	160 ± 19	796 ± 90
Cr	2.0 ± 0.3	0.21 ± 0.03	0.00	0.80 ± 0.11	1.1 ± 0.2	29 ± 3
Zn	28 ± 3	6.0 ± 0.8	10 ± 1	7.0 ± 1.1	137 ± 20	33 ± 4
P	0.00	0.00	0.00	0.00	7.0 ± 1.2	42 ± 6
Mn	57 ± 6	2.0 ± 0.2	0.60 ± 0.09	0.50 ± 0.07	0.20 ± 0.03	6.0 ± 0.5
V	0.46 ± 0.07	0.34 ± 0.05	0.00	0.20 ± 0.04	0.00	40 ± 6
Cu	2.3 ± 0.3	0.83 ± 0.14	3.0 ± 0.4	10 ± 1	10 ± 1	6.0 ± 0.9
Ni	30.3 ± 3.8	1.2 ± 0.2	1.0 ± 0.1	1.0 ± 0.2	6.0 ± 0.6	16 ± 2
Sr	4.0 ± 0.5	1.0 ± 0.2	8.0 ± 1.0	15 ± 2	65 ± 6	31 ± 4
Ba	0.70 ± 0.09	1.24 ± 0.17	3.0 ± 0.4	9.0 ± 1.2	53 ± 9	52 ± 8
Fe	416 ± 42	33 ± 4	76 ± 8	223 ± 25	107 ± 12	124 ± 13

Range (±).

Table 3
Composition data (ppm) for 17 chemical elements in aqueous extracts obtained from clinker samples.

	MilliQ	Acetate	HCl	HCl-H$_2$O$_2$	HNO$_3$	HF-HNO$_3$
Si	0.00	0.00	10 ± 1	67 ± 10	0.00	165 ± 20
Al	249 ± 29	137 ± 16	134 ± 20	115 ± 14	97 ± 12	227 ± 24
Ti	178 ± 22	21.7 ± 3.4	43.7 ± 5.5	32 ± 4	8.1 ± 1.4	1841 ± 233
Na	79 ± 11	12.5 ± 2.1	9.0 ± 1.5	27 ± 3	4.8 ± 0.5	6.0 ± 1.0
Mg	1474 ± 211	74 ± 11	5.2 ± 0.6	1.2 ± 0.2	17 ± 2	468 ± 39
Ca	473 ± 41	105 ± 13	144 ± 15	49 ± 7	102 ± 11	151 ± 19
K	502 ± 45	278 ± 28	245 ± 26	371 ± 33	226 ± 22	1385 ± 170
Cr	14 ± 2	0.66 ± 0.08	2.0 ± 0.3	1.1 ± 0.2	0.5 ± 0.1	24 ± 3
Zn	10 ± 1	3.0 ± 0.4	4.4 ± 0.5	0.00	63 ± 8	16 ± 2
P	68 ± 8	14 ± 2	0.00	319 ± 30	57 ± 6	230 ± 25
Mn	253 ± 26	23 ± 3	0.7 ± 0.1	4.0 ± 0.5	0.3 ± 0.1	12 ± 2
V	11 ± 1	3.1 ± 0.5	2.0 ± 0.3	0.8 ± 0.1	0.3 ± 0.0	13 ± 1
Cu	0.94 ± 0.15	0.13 ± 0.02	0.11 ± 0.01	0.40 ± 0.05	4.0 ± 0.6	3.1 ± 0.5
Ni	0.5 ± 0.1	0.41 ± 0.06	0.00	0.3 ± 0.0	0.6 ± 0.1	2 ± 0
Sr	6.4 ± 0.7	9.5 ± 1.0	2.1 ± 0.2	0.3 ± 0.0	0.9 ± 0.1	8.0 ± 1.1
Ba	9.1 ± 1.2	19 ± 2	27 ± 3	8.0 ± 0.9	4.0 ± 0.4	57 ± 6
Fe	505 ± 43	386 ± 35	86 ± 9	61 ± 7	60 ± 6	247 ± 26

Range (±).
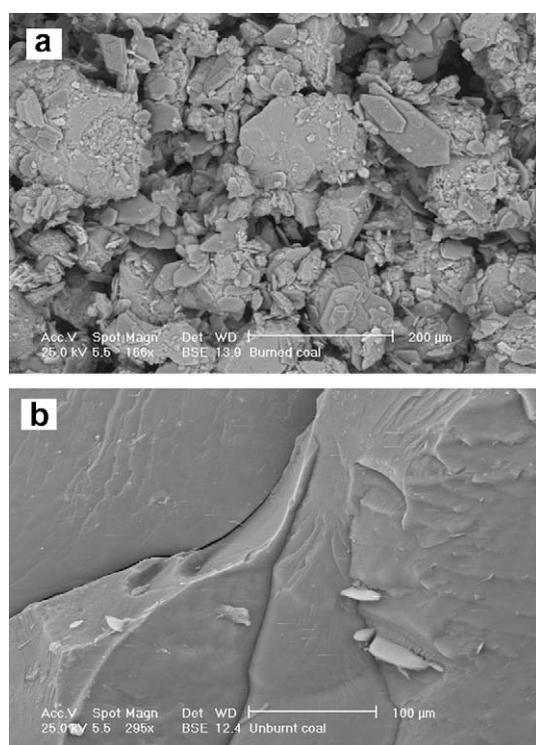
Fig. 2. Scanning electron photographs of fresh coal and clinker material: (a) SEM micrograph in BSE mode of clinker material shows lens-shaped nodules, (b) BSE image displays the morphology of unaltered coal.

Fig. 3. Relative percents of total extracted from fresh coal and clinker material for individual elements released during sequential procedure.

4.3. XRD analyses

The mineralogical composition of the clinker material and fresh coal samples has been analysed using XRD (see Fig. 4a for the results). An initial diffractogram corresponding to unaltered coal (acquired using a 0.05° scan step and a 1 s time step) did not allow the crystalline phases present to be easily distinguished. Therefore, a subsequent diffractogram was run with a 0.05° scan step and a 3 s time step. In neither diffractogram is it possible to distinguish any of the most common crystalline phases of unweathered coal (i.e., pyrite, dolomite, calcite, and others).

Further XRD analysis obtained directly from the thermally altered material showed a fairly complex composition. The major minerals identified were: quartz (85-0794); potassium hydrogen sulfate (46-0496), K(HSO$_4$); sodium hydrogen phosphate (09-0100), Na$_2$H$_2$(PO$_3$)$_4$; calcite (86-2341); and aluminum sulfate hydrate (49-1096), Al$_2$(SO$_4$)$_3$·16H$_2$O. Moreover, the following crystalline phases were also observed as minor compounds: magnetite (89-6466); sodium magnesium titanium oxide (37-0545), Na$_{0.7}$Ti$_{1.7}$Mg$_{0.4}$O$_4$; and chabazite-K (44-0250), KAlSiO$_4$·xH$_2$O. The presence of chabazite-K indicates that the vent from which the sample was taken reached temperatures no higher than 230 °C, the temperature at which this zeolite decomposes. The occurrence of magnetite and several sulfates have been previously reported in coal fires (Sokol et al., 1998; Heffern and Coates, 2004). In regards
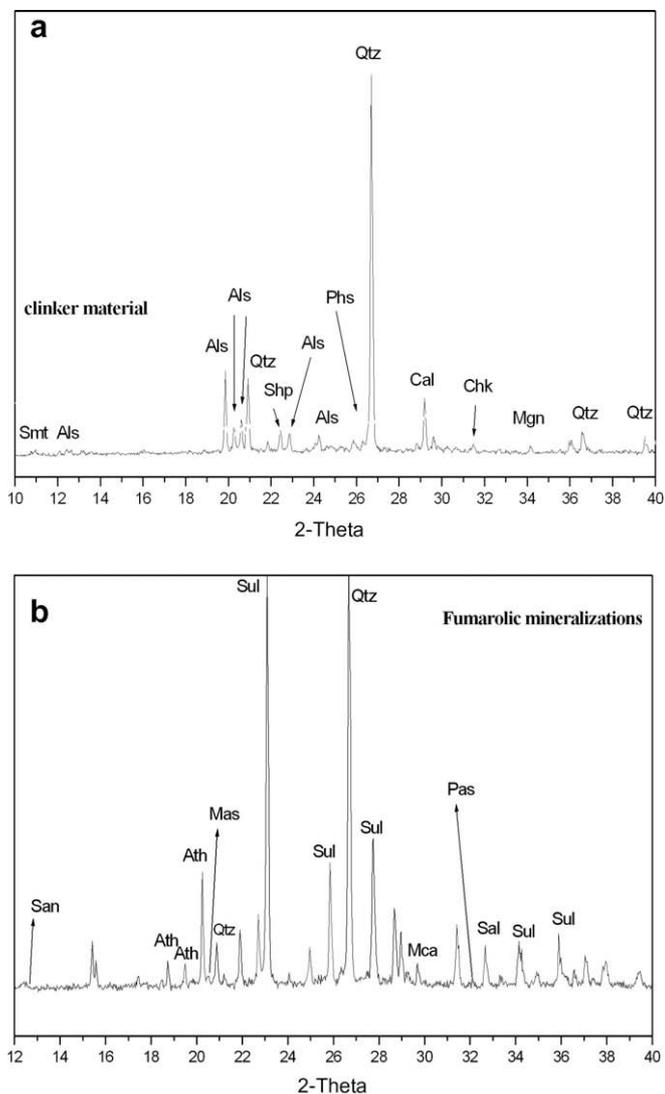
structures produced by rapid fragmentation and destruction of the unaltered carbon structure during self-oxidation (Fig. 3a). In contrast, the sample of fresh coal displays a compact texture in BSE mode (Fig. 3b). Both images show a uniform chemical composition for the two samples. Since the system loses almost all the volatile matter and much of the fixed carbon during self-oxidation, this loss of mass surely accounts for the textural changes observed (Bentor et al., 1981). The end product of the spontaneous oxidation is a clinker material with a predominantly rounded shape and possible scarcely melted textures, as compared to the low porosity that is typical of fresh coal (Cosca et al., 1989).

Fig. 4. (a) X-ray diffraction patterns showing the peaks corresponding to clinker material; (b) XRD data of the mineralizations, acquired applying a 0.05° step scan with a 1 s step time. Note: Qtz, quartz; Als, aluminum sulfate hydrate; Cal, calcite; Shp, sodium hydrogen phosphate; Mgn, magnetite; Phs, potassium hydrogen sulfate; Smt, sodium magnesium titanium oxide; Chk, chabazite-K; Sal, salammoniac; Sul, sulfur; Mas, mascagnite; San, sanidine; Ath, ammonium thiosulfate; Mca, magnesium calcite; Pas, potassium ammonium aluminum sulfate hydrate.

to the fumarolic mineralizations, X-ray diffraction data show the following mineralogical composition (Fig. 4b): quartz (86-1560); potassium ammonium aluminum sulfate hydrate (48-0243), $K_{0.5}(NH_4)_{0.5}Al(SO_4)_2 \cdot H_2O$; sulfur (78-1889); K-feldspar (79-0349), $H_{0.9}K_{0.1}(AlSi_3O_8)$; magnesium calcite (89-1306), $Ca_{0.9}Mg_{0.1}CO_3$; salammoniac (07-0007), NH_4Cl; mascagnite (76-0579), $(NH_4)_2SO_4$; and, finally, ammonium thiosulfate (31-0067), $(NH_4)_2S_2O_3$.

The dominant minerals derived from smoldering coal beds in the Cerro Pelado Formation are similar to phases detected at the principal burning coal seams in Pennsylvania (USA) and Gauteng (South Africa), among others (Stracher, 1995; Pone et al., 2007). Particularly worthy of note is the important presence of sulfur-bearing minerals and ammonium condensation by-products at the gas vents in the study outcrop of coal; this mineral assemblage suggests the mobilization of different components of the coal matrix, which were recombined with sulfate and other ions in the system.

It is revealed (Sokol et al., 1998) that salammoniac, different feldspars, magnesium phases, free sulfur and mascagnite are some

widespread material-forming minerals of products associated with oxidation of coal. The presence of salammoniac occurs as a sublimation product of gas jets and may, in part, be dissolved into the surface water (Pone et al., 2007). Elemental sulfur and other sulfate compounds are also interpreted to have been sourced from gaseous exhalations associated with alteration of coal; they all ultimately derive from sulfur oxides and are formed by interaction of gases exhaled from vents with surface water, and surrounding rocks (Stracher, 1995).

The three types (Calkins, 1994) into which sulfur in coal can be divided – pyritic sulfur, organic sulfur and sulfur in sulfate minerals – undergo a transformation during coal oxidation to produce sulfite and, hence, sulfate and thiosulfate (Mills et al., 1999). Moreover, mascagnite and ammonium thiosulfate could be derived from reaction between ammonium ions associated with salammoniac and sulfur-content ions in the aqueous phase. Specifically, ammonium thiosulfate could well have formed by the selective oxidation of the sulfur-content ions, favoured by certain metal oxides (Cho et al., 2002). Nonetheless, in crystalline form, ammonium thiosulfate is only stable at certain temperatures, a neutral or slightly alkaline pH, and low Eh values; it decomposes by oxidation to produce intermediate products comprising meta-stable sulfur compounds such as tetrathionates or trithionates and end products consisting of elemental sulfur and ammonium sulfate (Wan, 1997):

$$4S_2O_3^{2-} + O_2 = 4SO_4^{2-} + 4S$$
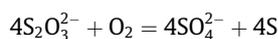
In addition, a greater amount of ammoniacal substances inhibits the decomposition of ammonium thiosulfate (Aylmore and Muir, 2001), whereas atmospheric oxygen favours the decomposition of the thiosulfate ion (Li and Miller, 1996):

$$5S_2O_3^{2-} + 2S_3O_6^{2-} + 10NH_4 + O_2 = 10NH_3 + 5H_2O + 4S_4O_6^{2-}$$
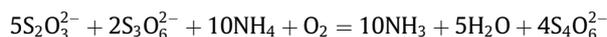
Finally, ammonium thiosulfate and potassium ammonium aluminum sulfate hydrate cannot be considered as valid minerals since the combustion products of coal beds are not generally regarded as mineral species (CNMMN, 1998). In addition, neither ammonium thiosulfate nor potassium ammonium aluminum sulfate hydrate are actually formed as minerals by other geological processes. However, both compounds have been reported as synthetic crystalline phases (Elerman et al.,1978; Smith, 1979; Troemel, 1997).

4.4. FTIR analysis

Ammonium thiosulfate was identified in a fumarolic mineralization sample using the XRD powder technique, and its IR absorption spectrum was analysed (Fig. 5). Several absorption bands were related to different compounds in agreement with reference data in the literature (Pretsch et al., 2000). The infrared spectrum of the analysed sample was useful in identifying ammonium sulfate, which shows absorption bands at 1088, 670, 614, and 464 cm^{-1}, characteristic of the sulfate and thiosulfate groups (vibrational modes of sulfur-oxygen bonds).

In particular, one band over 3000 cm^{-1} (3207 cm^{-1}) can be related to the ammonium ion (N–H stretching vibrations). The S–S characteristic absorption was also found for the sample with a peak at 532 cm^{-1}; this absorption can be due to a mode corresponding to thiosulfate group. The significant band around 1400 cm^{-1} can be assigned to $RO–SO_2–SR$ deformations; hence, this band indicates the presence of ammonium thiosulfate. With calcium carbonate, the position of the 1675 cm^{-1} band could correspond to a vibrational mode of carbon-oxygen double bonds belonging to the carbonate group. Finally, several distinguishable bands were also observed (979 and 798 cm^{-1}). These absorption bands and other overlapping ones (1087 and 464 cm^{-1}) are due to silicon-oxygen bond stretching vibrations related to quartz.
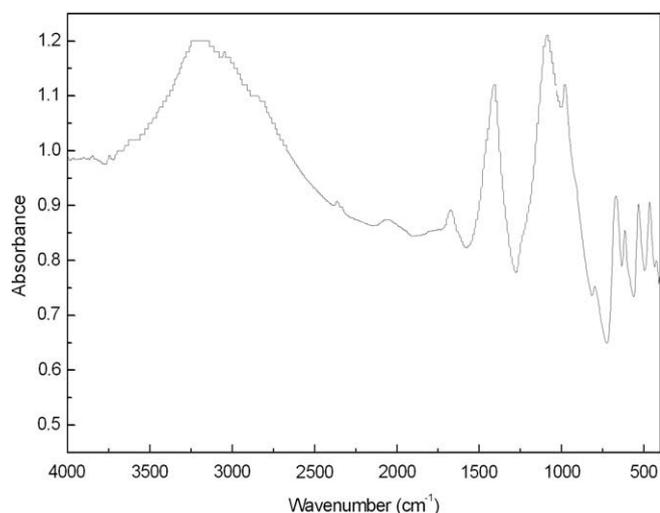
Fig. 5. FTIR absorption spectrum of fumarolic mineralizations.

Table 4
Average aliphatic hydrocarbons, ethane and aromatic compounds from the studied coal outcrop.

	Concentration (ppm)
Ethane	87.6
Propane	16.4
i-Butane	1.5
n-Butane	3.8
i-Pentane	0.9
n-Pentane	1.7
n-Hexane	1.0
n-Heptane	0.6
n-Octane	0.3
Ethene	10.9
Benzene	5.0
Toluene	3.9
m/p-xylene	0.2
o-xylene	0.2
Ethylbenzene	<0.1

Regarding the rest of the fumarolic mineralization samples, no considerable changes in FTIR spectra were observed.

4.5. Gas chromatographic analyses

Average values for all aliphatic hydrocarbons, ethene and the main aromatic compounds analysed from gas samples are shown in Table 4. Other analyses of gas samples revealed the presence of significant concentrations of methane (1345 ppm), carbon monoxide (480 ppm) and carbon dioxide (23,945 ppm). Finally, temperatures in the range from 180 °C to 210 °C were measured in gases escaping from vents.

The results for greenhouse and other gases indicate rather low concentrations when compared to those observed in gaseous effluents emitted from the Witbank coalfield, South Africa (Pone et al., 2007). Benzene and toluene were the major VOCs emitted from smoldering coal beds in the Cerro Pelado Formation; both aromatic compound contribution was approximately 95% of overall VOCs emitted. In contrast, the concentrations of aliphatic hydrocarbons were more regular than that of aromatic compounds; ethane contribution was 65% of the overall aliphatic hydrocarbons, followed by propane (13%) and ethene (8%). Finally, it was estimated that for oxidation of coal in "La Cuesta" mine, approximately 1.8 tonnes of carbon dioxide per tonne of coal was produced.

5. Conclusions

The integration of the geochemical, mineralogical, and textural results reveal that the self-oxidation of coal is quite a complex geochemical process. Since the system is open, generally immobile elements such as titanium and aluminum lixiviate at low pH, and elements such as phosphorous and nitrogen are concentrated. This process releases contaminating metals into the environment, such as Cr, Cu, Ni, and Zn, as well as the elements Mg, K, Ca, and Na.

The chemical analyses of the different extracts obtained by the sequential attacks on clinker and coal samples has revealed three basic groupings of the elements studied, based on their geochemical patterns during self-oxidation: (1) those that become quite mobile (Na, Sr, Cr, Ni, etc.); (2) those that undergo partial enrichment (Mg, Fe, V, K, etc); and (3) those that remain nearly immobile (Ti, P).

Spontaneous oxidation favours various crystalline phases as well, mainly sulfates, thiosulfates, phosphates, elemental sulfur, and hydrate aluminosilicates. The process also causes the coal to change from a compact texture to a rounded, much more porous texture. Consequently, the first natural occurrence of ammonium thiosulfate, a non-mineral crystalline phase previously obtained only synthetically, which decomposes at relatively low temperatures, can be explained by circumstances on the self-heating of the coal such as the environmental conditions, the high sulfur content and the inhibitory effect of large amounts of ammoniacal products.

Gas readings in several emissions from vents showed significant average contents of greenhouse gases, BTX and aliphatic hydrocarbons.

References

Anthony, J.W., Williams, S.A., Bideaux, R.A., 1977. Mineralogy of Arizona. University of Arizona Press, Tucson.
ASTM-American Society for Testing and Materials, 2002. ASTM D 3172-89: Standard Practice for Proximate Analysis of Coal and Coke. American National Standards Institute, Washington.
Audemard, F.A., 2003. Quaternary tectonics and present stress tensor of the inverted northern Falcón Basin, northwestern Venezuela. Journal of Structural Geology 23 (2/3), 431–453.
Audemard, F.A., Bousquet, J.C., Rodríguez, J.A., 1999. Neotectonic and paleoseismicity studies on the Urumaco Fault, northern Falcón Basin, northwestern Venezuela. Tectonophysics 308 (1/2), 23–35.
Aylmore, M.G., Muir, D.M., 2001. Thermodynamic analysis of gold leaching by ammoniacal thiosulfate using Eh/pH and speciation diagrams. Minerals and Metallurgical Processing 18 (4), 221–227.
Banerjee, S.C., 1985. Spontaneous combustion of Coal and Mine Fires. Balkema, Rotterdam. 165p.
Barletta, B., Meinardi, S., Simpson, I.J., Khwaja, H.A., Blake, D.R., Rowland, F.S., 2002. Mixing ratios of volatile organic compounds – VOCs – in the atmosphere of Karachi, Pakistan. Atmospheric Environment 36 (20), 3229–3443.
Bentor, Y.K., Kastner, M., Perlman, I., Yellin, Y., 1981. Combustion metamorphism of bituminous sediments and the formation of melts of granitic and sedimentary composition. Geochimica et Cosmochimica Acta 45 (11), 2229–2251.
Boesi, T., Goddard, D., 1991. A new geology model related to the distribution of hydrocarbon source rocks in the Falcón Basin, northwestern Venezuela. American Association of Petroleum Geology Memoirs 52, 303–319.
Bouska, V., 1981. Geochemistry of Coal. Elsevier Scientific Publishing Company, Prague. 350p.
Calkins, W.H., 1994. The chemical forms of sulfur in coal: a review. Fuel 73 (4), 475–484.
Carras, J.N., Young, B.C., 1994. Self-heating of coal and related materials, models application and test methods. Progress in Energy and Combustion Science 20 (1), 1–15.
Ceglarska-Stefanska, G., Brzóska, K., Winnicki, J., 1998. Sorption of water vapour on exinite concentrations. Chemistry and Materials Science 4 (3), 313–319.
Chakravorty, R.N., Kolada, R.J., 1988. Prevention and control of spontaneous combustion in coal mines. Mining Engineering 40, 952–956.

Chaterjee, R.S., 2006. Coal fire mapping from satellite thermal IR data, a case example in Jharia coaldfield, Jharklhand, India. Journal of Photogrammetry and Remote Sensing 60 (2), 113–128.

Cho, Y.G., Park, D.W., Park, D.G., Woo, H.C., Chung, J.S., 2002. Selective oxidation of hydrogen sulfide to ammonium thiosulfate and sulfur over vanadium-bismuth oxide catalysts. Research on Chemical Intermediates 28 (5), 419–431.

CNMMN-Commission on New Minerals and Mineral Names, 1998. Procedures and Guidelines on Mineral Nomenclature. International Mineralogical Association, Vandoeuvre lès Nancy.

Coates, D.A., 1991. Clinker. In: Morrison, R.B. (Ed.), Quaternary Nonglacial Geology. Conterminous US, The Geology of North America, vol. K-2. Geologic Society of America, Boulder, pp. 1–19.

Coates, D.A., Heffern, E.L., 2000. Origin and geomorphology of clinker in the Powder River Basin, Wyoming and Montana. In: Miller, R. (Ed.), Coal Bed methane and Tertiary Geology of the Powder River Basin. 50th Annual Field Conference Guidebook. Wyoming Geological Association, Casper, pp. 211–229.

Colman, J.J., Swanson, A.L., Meinardi, S., Sive, B.C., Blake, D.R., Rowland, F.S., 2001. Description of the analysis of a wide range of volatile organic compounds in whole air samples collected during PEM-Tropics A and B. Analytical Chemistry 73 (15), 3723–3731.

Cosca, M.A., Essene, E.J., Geissman, J.W., Simmons, W.B., Coates, D.A., 1989. Pyrometamorphic rocks associated with naturally burned coal beds, Powder River Basin, Wyoming. American Mineralogist 74 (1/2), 85–100.

Díaz de Gamero, M.L., 1977. Stratigraphy and micropaleontology of oligocene and early miocene in central Falcon Basin. Geos 22 (1), 3–60.

Díaz de Gamero, M.L., Linares, O.J., 1989. Stratigraphy and paleontology of the Urumaco Formation from the upper Miocene in northwestern Falcon State. VII Congreso Geológico Venezolano, Mem. I, Maracaibo, pp. 419–438.

Elerman, Y., Uraz, A.A., Armagan, N., Aka, Y., 1978. Crystal data for ammonium thiosulphate: (NH$_4$)$_2$S$_2$O$_3$. Journal of Applied Crystallography 11 (6), 709.

Escobar, M., Martínez, M., 1993. Geochemical and petrographic characteristics of the most important Venezuelan Coalfields. Interciencia 18 (2), 62–70.

Finkelman, R.B., 1999. Trace elements in coal, environmental and health significance. Biological Trace Element Research 67 (3), 197–204.

Finkelman, R.B., 2004. Potential health impacts of burning coal beds and waste banks. International Journal of Coal Geology 51 (1), 19–24.

Glasser, D., Bradshow, S.M., 1990. Spontaneous combustion combustion in beds of coal. In: Cheremisin, N. (Ed.), Handbook of Heat and Mass Transfer 4, Advances in Reactor Design and Combustion Science. NJ Gulf, Denver, pp. 1–9 (Chapter 26).

Gleit, A., 1986. Coal Sampling and Analysis, Methods and Models. Noyes Publishing, New Jersey. 188p.

González de Juana, C., Iturralde de Arozena, J., Picard, X., 1980. Geology of Venezuela and the Petroliferous Venezuelan Basins, vols. I & II. Fonvises ed., Caracas, 1031 p.

González, E., Nieves, G., Torrealba, N., 1985. Geological characteristics of the Cerro Pelado carboniferous basin. VI Congr. Geol. Venez., Mem. 6, Caracas, pp. 3966–3998.

Hambalek, N., Rull, V., Di Giacomo, E., Díaz de Gamero, M.L., 1994. Paleoecological and paleoenvironmental evolution of the sequence from the Neogene in the Urumaco Surco, palynological and lithological survey. Boletín de la Sociedad Venezolana de Geólogos 191 (1), 7–19.

Heffern, E.L., Coates, D.A., 2004. Geologic history of natural coal-bed fires in Powder River Basin. International Journal of Coal Geology 59 (1), 25–47.

Hudak, P.F., 2002. Spontaneous combustion of shale spoils at a sanitary lansfill. Waste Management 22 (7), 687–688.

Kaymakci, E., Didari, V., 2002. Relations between coal properties and spontaneous combustion parameters. Turkish Journal of Engineering and Environmental Science 26 (1), 59–64.

León, M.P., 1992. Fires in Coal Mines. Spanish Geological Survey, Madrid. 171p.

Li, J., Miller, J.D., 1996. Important solution chemistry factors that influence the copper-catalyzed ammonium thiosulfate leaching of gold. In: 125th SME Annual Meeting. Arizona, pp. 1–20.

Limacher, D., 1963. A propos de la formation de minéraux lors de la combustion des charbons. Societe Geologique du Nord, Annales 83 (Part 4), 287–288.

Lyman, R.M., Volkmer, J.E., 2001. Pyrophoricity -spontaneous combustion- of Powder River Basin coals, considerations for coal-bed methane development. Geo-Notes No. 69, Wyoming State Geological Survey, Laramie, pp. 18–22.

Martínez, M., Escobar, M., Esteves, I., López, C., Galárraga, F., González, R., 2001. Trace elements of Paleocene Táchira coals, southwestern Venezuela, a geochemical study. Journal of South American Earth Sciences 14 (4), 387–399.

McCarty, D.K., Moore, J.N., Marcus, A.W., 1998. Mineralogy and trace elemental association in an acid mine drainage iron oxide precipitate: comparison of selective extractions. Applied Geochemistry 13, 165–176.

Mills, C., Robertson, A., Shaw, S., 1999. The Role of Microorganisms in Acid Rock Drainage. InfoMine Inc., Vancouver.

Palmer, C.A., Krasnow, M.R., Finkelman, R.B., d'Angelo, W.M., 1993. An evaluation of leaching to determine modes of occurrence of selective toxic elements in coal. Journal of Coal Quality 12 (4), 135–141.

Pone, J.D., Hein, K.A., Stracher, G.B., Annergarn, H.J., Finkelman, R.B., Blake, D.R., McCormack, J.K., Schroeder, P., 2007. The spontaneous combustion of coal and its by-products in the Witbank and Sasolburg coaldfields of South Africa. International Journal of Coal Geology 72 (2), 124–140.

Pretsch, E., Buhlmann, P., Affolder, C., 2000. Structure Determination of Organic Compounds and Tables of Spectral Data. Springer-Verlag Publishing, New York.

Puttmann, W., Steffens, K., Globel, W., 1991. Analysis of aromatic hydrocarbons in overburden from coal mines, assessment of the environmental impact. In: Peters, D.C. (Ed.), Geology in Coal Resource Utilization. Techbooks, Fairfax, pp. 483–498.

Rosema, A., Guan, H., Veld, H., 2001. Simulation of spontaneous combustion, to study the causes of coal fires in the Rujigou Basin. Fuel 80 (1), 7–16.

Sarnecki, J.C., 1991. Formation of clinker and its effects on locating and limiting coal resources. In: Peters, D.C. (Ed.), Geology in Coal Resource Utilization. Techbooks, Fairfax, pp. 29–35.

Smith, G.W., 1979. Crystal data for ammonium thiosulphate (NH$_4$)$_2$S$_2$O$_3$. Journal of Applied Crystallography 12 (2), 246.

Sokol, E., Volkova, N., Lepezin, G., 1998. Mineralogy of pyrometamorphic rocks associated with naturally burned coal-bearing spoil-heaps of the Chelyabinsk coal basin, Russia. European Journal of Mineralogy 10 (5), 1003–1014.

Stracher, G.B., 1995. The anthracite smokers of eastern Pennsylvania, P$_{S2(g)}$ stability diagram by TL analysis. Mathematical Geology 27 (4), 499–511.

Stracher, G.B., Taylor, T.P., 2004. Coal fires burning out of control around the world: thermodynamic recipe for environmental catastrophe. International Journal of Coal Geology 59 (1), 7–17.

Stracher, G.B., Taylor, T.P., Nolter, M., Vice, D.H., Blake, D.R., Cerpovicz, P., 2004. Centralia mine fire collecting extravaganza with National Geographic. Geological Society of America, Abstracts with Programs 36 (5), 42.

Troemel, M., 1997. Various Oxides. ICDD Grant-in-Aid, Frankfurt.

Walker, S., 1999. Uncontrolled Fires in Coal and Coal Wastes. The Clean Coal Centre, London. 73p.

Wan, R.Y., 1997. Importance of Solution Chemistry for Thiosulfate Leaching of Gold. World Gold Conference, Singapore. pp. 159–162.

Wang, H., Dlugogorski, B.Z., Kennedy, E.M., 2003. Coal oxidation at low temperatures: oxygen consumption, oxidation products, reaction mechanism and kinetic modeling. Progress in Energy and Combustion Science 29 (6), 487–513.